Nano-sized iron oxide with controlled size modified with Pd for purification processes

S. Zh. Todorova[1]*, Z. P. Cherkezova-Zheleva[1], I. D. Yordanova[1], A. Ganguly[4],
H. G. Kolev[1], S. Mondal[2], M. G. Shopska[1], K. K. Tenchev, N. I. Velinov[1],
A. K. Ganguli[2,3,4], G. B. Kadinov[1]

[1] *Institute of Catalysis, Bulgarian Academy of Sciences, Acad. G. Bonchev St.,
Block 11, 1113 Sofia, Bulgaria*
[2] *Department of Chemistry, Indian Institute of Technology, Hauz Khas, New Delhi 110016, India*
[3] *Nanoscale Research Facility, Indian Institute of Technology, Hauz Khas, New Delhi 110016, India*
[4] *Institute of Nano Science & Technology, Habitat Centre, Phase – X, Mohali, Punjab, 160062, India*

Fe_3O_4 nano-oxide was prepared by wet chemical procedure and it was modified with palladium. The catalysts were characterized by X-ray diffraction (XRD), X-ray photoelectron spectroscopy (XPS), transmission electron microscopy (TEM), temperature programmed reduction (TPR) and diffuse reflectance infrared spectroscopy (DRIRS).

The catalytic performance of Fe_2O_3 and Pd/Fe_2O_3 was examined in the reaction of CO oxidation. Strong interaction between palladium and the nano-sized oxide was established leading to the formation of finely divided PdO on the surface. Remarkable increase in the catalytic activity was found after Fe_2O_3 modification with Pd. This feature was explained with the ability of the iron oxide, located in the close proximity to palladium, to provide active oxygen species that can subsequently react with CO molecules adsorbed on adjacent Pd. The Langmuir–Hinshelwood reaction mechanism of CO oxidation was suggested to proceed up to 100 °C over Pd/Fe_2O_3 catalyst including both the linear and bridge-bonded CO.

Key words: iron nano-oxide, palladium modified iron oxide, CO oxidation.

INTRODUCTION

The iron oxide nano-particles are of considerable interest due to their wide range of applications in chemical industries, magnetic storage materials, medicine and environmental protection [1]. Considering numerous applications of the iron oxides in various emerging fields, remarkable efforts on the synthesis of nano-dispersed particles are continuing. The biggest challenge in this field is to economically produce iron oxide nano particles of desired characteristics for specific application in large scale. There is a lot of progress in understanding the basic science of the nano-iron oxides but the evaluation of their catalytic properties and industrial application needs much more attention [2]. The application of the nano-sized iron oxides can be attributed to the difference in properties of the particles in nano scale as compared to their bulk counterparts. The iron oxide materials have been found to be good candidates as cheap and efficient catalysts, especially in environmental processes [3, 4]. The magnetite and hematite are the most applied iron oxides as catalysts for oxidation/reduction and acid/base reactions. The nano-particle iron oxide is significantly more effective than conventional micronsized iron oxide for the oxidation of CO [5]. These effects could be derived from the high activity of the nano-particles that have high BET surface area and more coordination unsaturated sites on the surfaces. Chemical and electronic properties, such as phase changes, OH content, band gap changes etc., could also contribute to their high reactivity [4]. Fe_2O_3 based nano-materials have been developed for the selective catalytic reduction (SCR) of NOx by NH_3 in diesel exhaust [6]. The catalytic activity of nano-sized Pd/Fe_2O_3 and Au/Fe_2O_3 at low temperatures in a CO oxidation reaction has been investigated [7, 8]. The activity of Pd/Au in the reaction of CO oxidation depends of the active phases' particle size,

* To whom all correspondence should be sent:
E-mail: todorova@ic.bas.bg

morphology, and Pd (Au)–support interactions. On the other hand Pd supported catalysts are widely accepted as the most active catalysts for catalytic combustion of methane and the low temperature oxidation of CO [7].

The present work aimed development of highly active and stable catalysts for CO oxidation by appropriate combination of Pd and iron nano-oxide with controlled size, shape and morphology.

2. EXPERIMENTAL

2.1. Samples preparation

The iron oxide was prepared according to the procedure described in [9]. Before Pd deposition the metal oxide was calcined 2 h at 450 °C in air. The as-prepared iron oxide was modified with Pd (~0.5% wt. Pd) by impregnation with aqueous solution of $Pd(NO_3)_2.2H_2O$. The quick evaporation of the solvent after the impregnation step was applied [10]. Thus the oxide particles were coated by a thin layer of Pd. The sample was calcined additionally for 2 h at 450 °C in air.

2.2. Catalysts characterization

The XRD patterns were obtained on TUR M62 apparatus, HZG-4 goniometer with Bregg-Brentano geometry, Co Kα radiation and Fe filter. XRD data processing was performed by using the X'Pert HighScore program. The HRTEM studies were carried out using FEI Technai G2 20 (200 kV). The TEM samples were prepared by loading an ethanol suspension of the sample on a holey copper grid. The specific surface area of supported catalyst samples have been determined by low temperature adsorption of nitrogen according to the B.E.T. method using Nova 1200 (Quantachrome) apparatus. The samples were degassed for 4–6 hours between 70–150 °C prior to the measurement. Temperature-programmed reduction (TPR) was carried out using a flow mixture of 10% H_2 in Ar at 10 ml/min, temperature rate of 10 °C/min up to 700 °C. Prior to the TPR experiment, the samples were treated in Ar for 1 hour at 150 °C.

The Mössbauer spectra were obtained at room temperature with an electromechanical spectrometer (Wissenschaftliche Elektronik GMBN, Germany) working in a constant acceleration mode. A ^{57}Co/Rh source (activity ≈ 50 mCi) and α-Fe standard were used. The experimentally obtained spectra were subjected to mathematical processing according to the least squares method. The parameters of hyperfine interaction such as isomer shift (IS), quadrupole splitting (QS) and magnetic hyperfine field (Hhf) as well as the line widths (FWHM) and the relative spectral area (G) of the partial components of the spectra were determined.

X-ray photoelectron measurements were carried out on the ESCALAB MkII (VG Scientific) electron spectrometer at a base pressure in the analysis chamber of 5×10^{-10} mbar using twin anode MgKα/AlKα X-ray source with excitation energies of 1253.6 and 1486.6 eV, respectively. The spectra were recorded at the total instrumental resolution (as it was measured with the FWHM of $Ag3d_{5/2}$ photoelectron line) of 1.06 and 1.18 eV for MgKα and AlKα excitation sources, respectively. The energy scale was calibrated by normalizing the C1s line of adsorbed adventitious hydrocarbons to 285.0 eV. The processing of the measured spectra includes a subtraction of X-ray satellites and Shirley-type background. The peak positions and areas were evaluated by a symmetrical Gaussian-Lorentzian curve fitting. The relative concentrations of the different chemical species were determined based on normalization of the peak areas to their photoionization cross-sections, calculated by Scofield [11].

The adsorption of CO on Pd/Fe_2O_3 catalyst was studied by *in situ* diffuse reflectance infrared Fourier transform (DRIFT) spectroscopy, using a Nicolet 6700 spectrometer equipped with a high temperature/vacuum chamber installed in the Collector II accessory (Thermo Spectra-Tech). The CO was adsorbed from $CO+N_2$ or $CO+O_2+N_2$ flow mixture at room temperature. Experiments were carried out on oxidized ("as-prepared", pretreated in N_2 for 1 h at 350°) surface.

2.3. Catalytic activity measurements

The catalytic tests were carried out in a flow type glass reactor at atmospheric pressure with a catalyst loading of about 0.5 cm³ (fraction 0.25–0.31 mm). The gas mixture consisted of 1700 ppm CO, 2 vol.% O_2 and He for balance to 100 vol.%. External mass transfer limitations were minimized by working at high GHSV (60 00 h⁻¹). The reaction temperature was measured by an internal thermocouple. The gas analysis was performed by a HP5890 series II gas chromatograph equipped with a thermal conductivity detector and Carboxen-1000 column. Helium was used as a carrier gas.

3. RESULTS AND DISCUSSION

The powder X-ray diffraction studies of the oxide nanoparticles show the formation of a cubic phase for iron oxide (PDF 01-080-153 9) (Figs 1 and 2).

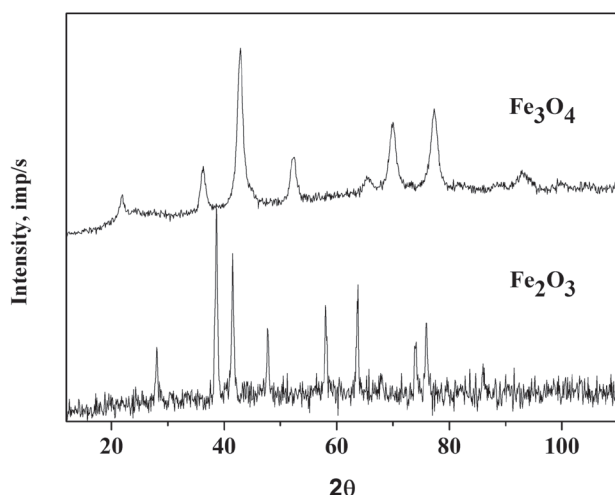The size and morphology of the oxide nanoparticles were found out from the TEM images of

Fig. 1. XRD pattern of non calcinated Fe_3O_4 and after calcination
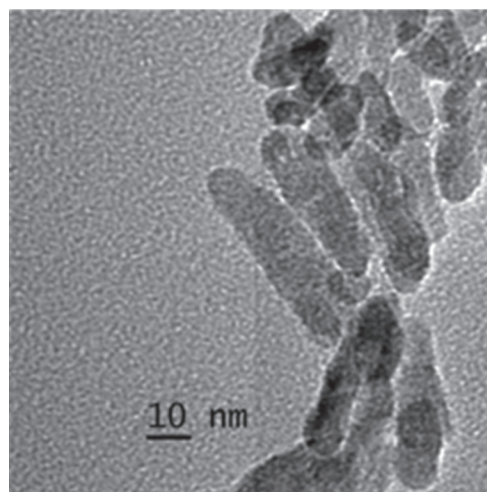

Fig. 2. TEM image of Fe_3O_4 before calcination

the oxide sample, the formation of particles of size elongated nanostructures of iron oxide with diameter ~12 nm and length ~50 nm. This oxide material is characterized by high surface area of 97 m^2/g.

According to the XRD data, the calcination in air leads to transformation of Fe_3O_4 to Fe_2O_3 and to an increase in the particles mean diameter about two times. The palladium deposition and following calcination do not increase the particle size additionally (Table 1). Decrease in the specific surface area was observed for an iron oxide sample after treatment in air for 2 h at 450 °C. Palladium or palladium oxide
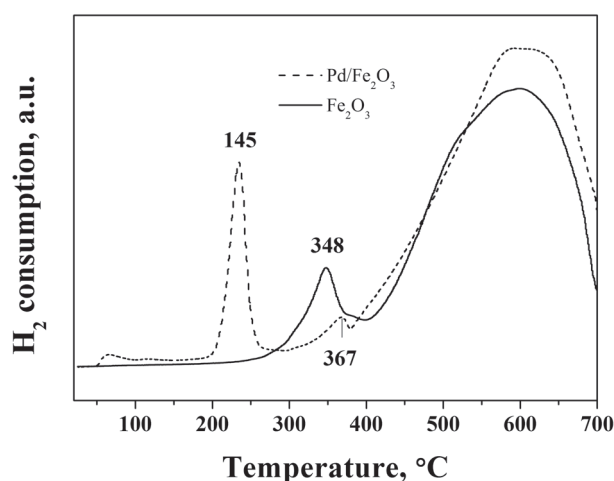
Table 1. Samples characterization after calcination

Sample	D_{MeOx}, [nm]	$S_{BET,}$ [m^2/g]
Fe_2O_3	22	28.8
0.5Pd/Fe_2O_3	22	27

were not detected in XRD spectrum of Pd modified sample revealing finely divided phase of palladium (XRD data are not given).

TPR spectra of Fe_2O_3 after calcination and of the oxide after Pd loading are presented on the Figure 3.

TPR profile of the Fe_2O_3 (Fig. 3) shows sharp reduction peak at 348 °C, attributed to the reduction of Fe_2O_3 to Fe_3O_4, and a broad peak in the temperature interval 450–700 °C, assigned to the subsequent reduction of Fe_3O_4 to FeO and Fe [12]. The reduction of Fe_2O_3 to Fe_3O_4 in Pd/Fe_2O_3 takes place at signifi-

Fig. 3. TPR profile of Fe_2O_3 and Pd/ Fe_2O_3

cantly lower temperature. It is well known that addition of a noble metal to oxide catalysts accelerates the reduction of the oxides by supplying hydrogen via spillover from the pre-reduced noble metal particles to the oxides [13]. Three major reduction peaks are detected during the reduction of the Pd/Fe_2O_3 sample. The peak located at lower temperature is attributed to the reduction of the metal oxide in contact with the Pd metal particles, and the peak located at higher temperature is assigned to the reduction of the large oxide particles apart from the noble metal particles [14]. Since PdO can be reduced at very low temperature, it should be noted that a separate peak corresponding to the reduction of Pd oxide, only, was not observed in our experiments. This is due to the low Pd content (high FeOx/Pd ratio) in our cata-

lysts leading to very small hydrogen consumption by palladium compared to that one for the reduction of iron oxide.

Moessbauer spectra of prepared ferrite powders registered at room temperature are presented on Figure 4. The spectrum A of the initial material (Fe_3O_4) is superposition of sextet and doublet components. Sextet lines, only, are registered in Möessbauer spectra of the other two samples Fe_2O_3 (spectrum B) and Pd/Fe_2O_3 (spectrum C) which are thermally treated iron oxide powder and that after Pd deposition, respectively. The calculated Moessbauer parameters after the best computer fitting of the spectra with respective components are given in Table 2. The calculated hyperfine parameters of the sextet components in the spectrum of the initial material (spectrum A) could be attributed to the presence of highly disperse ferrite phase with particle size bellow 20 nm showing collective magnetic excitation (CME) behaviour [1, 15, 16].

In this spectrum (of Fe_3O_4) iron ions in octahedral and tetrahedral position in spinel particles are distinguished. The calculated hyperfine parameters of doublet components could be attributed to the presence of ferrite particles with superparamagnetic (SPM) behaviour and ultra-disperse size bellow 10 nm [1. 15, 16]. The calculated hyperfine parameters of the sextet components in the other two spectra (Fe_2O_3 (spectrum B) and Pd/Fe_2O_3 (spectrum C)) could be attributed to the presence of bulk hematite particles and (compare G column 66/72%) and hematite particles with lower size (compare G column 33/28%) (see Table 2).

The oxidation states of Pd and Fe on the catalytic surface were studied by X-ray photoelectron spectroscopy.

The Pd3d and Fe2p XP spectra of $0.5\%Pd/Fe_2O_3$ are shown in Fig. 5. The line form, position of the peak and the position of satellite structures for Fe2p XP spectra were compared with previously reg-
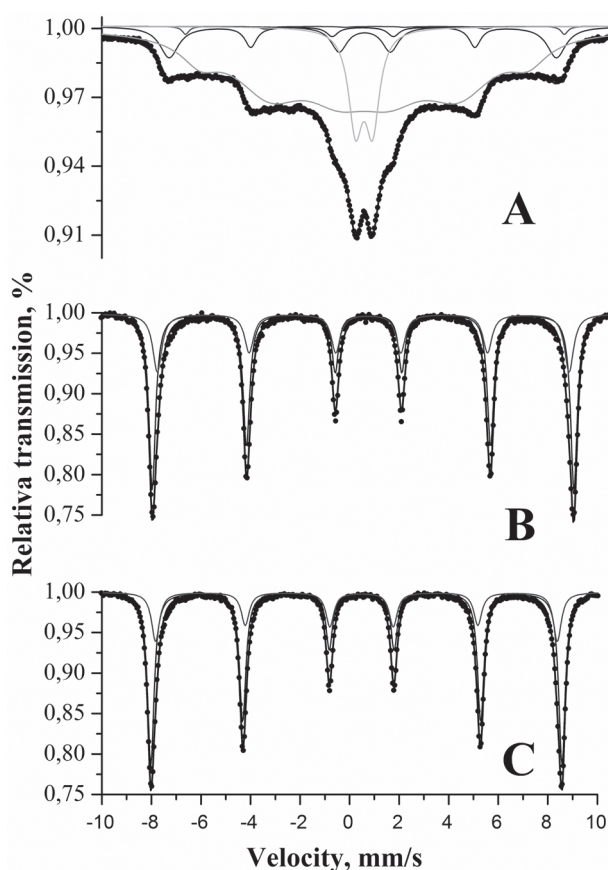

Fig. 4. Moessbauer spectra of synthesized materials. A − Fe_3O_4 − as synthesized initial sample; B − Fe_2O_3 − calcined initial sample; C − $0.5\%Pd/Fe_2O_3$

istered iron oxide spectra and with literature data also. Base on this we suggest the presence of Fe_2O_3 as a main phase [17]. Very weak satellite structure at binding energies about 719 eV (typical for Fe^{3+}) and $Fe2p_{3/2}$ peak at about 710.5 eV are characteristic for Fe^{3+}. The broadening of $Fe2p_{3/2}$ peak corre-

Table 2. Moessbauer parameters of the samples

| Sample	Components	IS, mm/s	QS, mm/s	H_{eff}, T	FMHW, mm/s	G, %
Fe_3O_4 (A)	Sxt 1 − Fe^{3+}_{tetra} spinel	0.27	0	47.3	0.75	9
	Sxt 2 − $Fe^{2.5+}_{octa}$ spinel	0.74	0	46.3	0.51	10
	Sxt 3 − Fe^{3+} − spinel CME	0.32	0	40.1	2.20	65
	Dbl 1 − Fe in spinel SPM	0.34	0.67	–	0.75	11
	Dbl 1 − Fe in spinel SPM	0.32	1.2	–	0.63	5
Fe_2O_3 (B)	Sxt 1 − Fe^{3+} in hematite	0.38	−0.21	51.5	0.32	66
	Sxt 2 − Fe^{3+} in hematite	0.37	−0.20	50.3	0.42	34
Pd/Fe_2O_3 (C)	Sxt 1 − Fe^{3+} in hematite	0.38	−0.21	51.5	0.31	72
	Sxt 2 − Fe^{3+} in hematite	0.37	−0.20	50.4	0.38	28
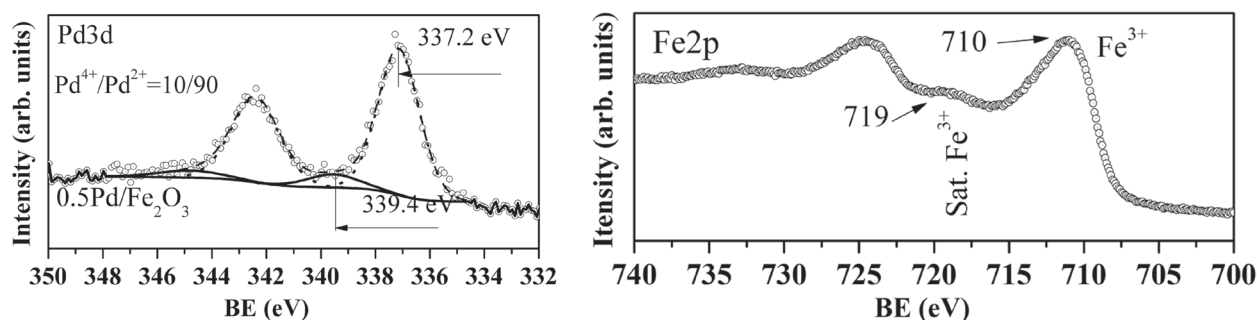
Fig. 5. XP spectra of Pd 3p and Fe 2p of 0.5%Pd/Fe$_2$O$_3$ after calcination 2 h at 450 °C

sponds to the presence of nano-sized particles. The surface atomic concentrations obtained from the normalized peak area divided by the cross section of the elements presented are as follow: Pd – 2 at.%; Fe – 33 at.%; and O – 65 at.%.

The binding energies in the range of 337.2–337.6 eV for Pd modified sample indicate the presence of PdO [18, 19]. A third component at 339.4 eV was observed. It is smaller than the other component detected and contributes with 10 % of the total Pd signals. This peak may be associated with Pd^{4+} from PdO$_2$ [19]. Pd^{4+} from PdO$_2$ is highly unstable, but according to Barr [20] Pd metal particles exposed long enough to air form on their surface PdO oxide with outermost layers of PdO$_2$ or Pd(OH)$_4$.

Figure 6 shows the CO conversion vs. temperature on the samples of iron oxide and iron oxide modified with palladium. The pure Fe$_2$O$_3$ demonstrate activy in CO oxidation. The addition of Pd results in remarkable displacement of the conver-
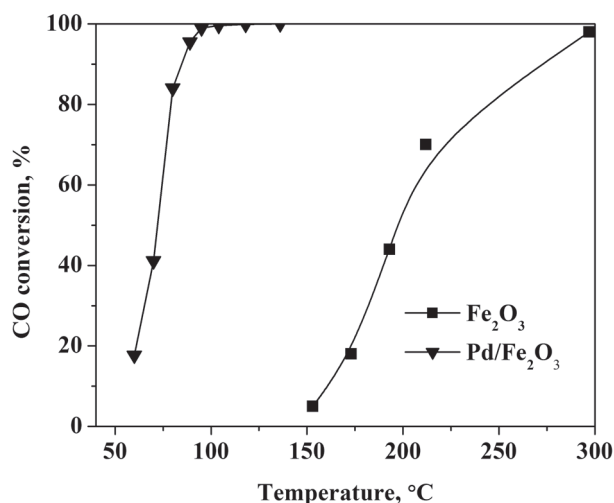
sion curve to lower temperature, indicating better catalytic activity (Fig. 6).

As it was mentioned above palladium presents at the catalyst surface as finely divided particles (there were no diffraction peaks for Pd nor PdO in the XRD spectrum) and palladium and iron oxide are supposed to interact strongly. According to Liu *et al.* [21] the promoting effect of iron oxide in the case of Pt-FeO$_x$ catalysts is related to the ability of the iron oxide species, located in close proximity to the palladium, to provide adsorption sites for oxygen that can subsequently react with CO molecules adsorbed on adjacent Pd sites. Thus, we can conclude that because of the high dispersion of Pd and close interaction between Pd and Fe$_2$O$_3$ in Pd/Fe$_2$O$_3$ sample, more surface oxygen species are provided to the palladium, thus improving its catalytic activity.

In situ DRIFT spectroscopy was used as one of the most powerful methods to obtain information about the type of the active sites, their stability and reactivity, chemical state of the surface under static and dynamic conditions in a wide temperature interval and after different pretreatments. DRIFT experiments on CO adsorption and reaction in O$_2$ –containing flow mixture were carried out to shed some light on the reaction mechanism.

The bridge-bonded CO band (at 1984 cm^{-1}) and linearly bonded CO on Pd^{1+} (at 2124 cm^{-1}) and Pd^0 (at 2089 cm^{-1}) are visible in the IR spectrum of Pd/Fe$_2$O$_3$ at T$_{room}$ (Fig. 7). The decrease in intensity of the bands of gas phase CO indicates activity in the CO oxidation even at ambient temperature. The bands of linearly and bridge-bonded CO are seen in the spectra collected up to 100 °C. The Langmuir–Hinshelwood mechanism (L-H) between adsorbed CO and oxygen species was well established as the dominant reaction pathway in the reaction of CO oxidation on noble metals [22]. Based on this it is possible to suggest that the reaction mechanism is L-H includes these two types of adsorption species. The so-called bi-functional reaction path involv-
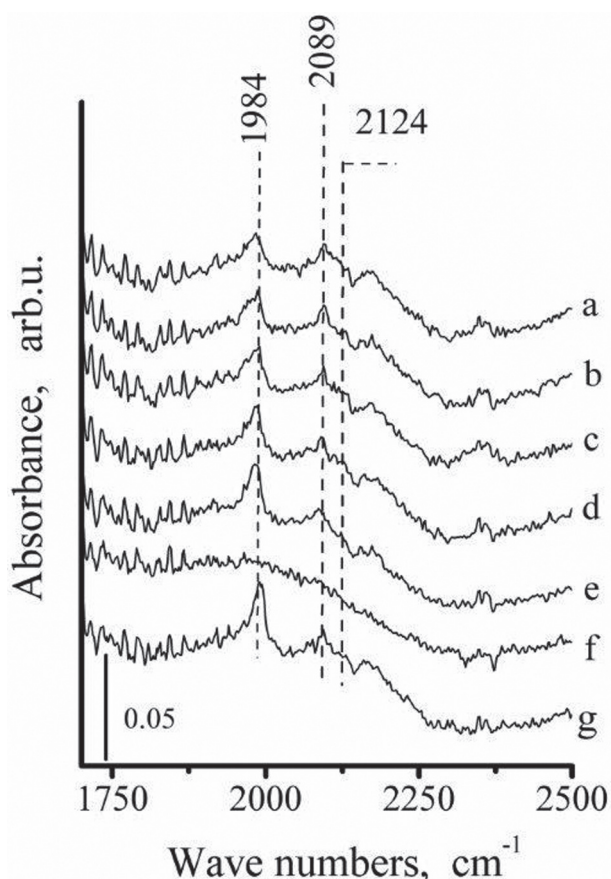

Fig. 6. Catalytic activity of the samples in the reaction of CO oxidation

Fig. 7. DRIFT spectra of CO adsorption in (1% CO + 10% O_2)/N_2 flow on Pd/Fe_2O_3 at different temperatures: **a**. N_2–O_2 flow at T_{room}; **b**. after 10 min, T_{room}; **c**. at 50 °C; **d**. at 70 °C; **e**. at 100 °C; **f**. at 150 °C; **g**. after cooling the sample in the reaction flow mixture at T_{room}

ing the reaction between CO adsorbed on the noble metal and oxygen from oxides is possible as well.

CONCLUSIONS

Strong interaction between the palladium and the nano-sized Fe_2O_3 oxide was established in a Pd/Fe_2O_3 catalyst leading to the formation of finely divided PdO on the surface. The high catalytic activity was established for Pd/Fe_2O_3 and it was explain with the ability of the iron oxide, located in close proximity to the palladium, to provide adsorption sites oxygen that can subsequently react with CO molecules adsorbed on the adjacent Pd.

Based on DR IRS investigations the Langmuir–Hinshelwood reaction mechanism was suggested for CO oxidation up to 100 °C over Pd/Fe_2O_3. The linear and bridge-bonded CO take part in the reaction on the surface of Pd/Fe_2O_3.

REFERENCES

1. U. Schwertmann, R. Cornell, Iron Oxides in the Laboratory, Weinheim, New York-Basel-Cambridge, 1991.
2. Anil K. Kandalam, B. Chatterjee, S.N. Khanna, B. K. Rao, P. Jena, B. V. Reddy, *Surf. Sci.*, **601**, 4873 (2007).
3. M. Mohapatra, S. Anand, *Int. J. Eng. Sci. Technol.*, **2**, 127 (2010).
4. S. C. Kwon, M. Fan, T. D. Wheelock, B. Saha, Sep. *Purif. Technol.*, **58**, 40 (2007).
5. J. S. Walker, G. I. Stragauzzi, W. H. Manogue, G. C.A. Schuit, *J. Catal.*, **110**, 298 (1988).
6. N. Apostolescu, B. Geiger, K. Hizbullah, M. Jan, S. Kureti, D. Reichert, F. Schott, W. Weisweiler, *Appl. Catal. B: Environ.*, **62**(1-2), 104 (2001).
7. M. Jin, J.-N. Parka, J. Shona, J. Kima, Z. Li, Y. Park, J. Kima, *Catal. Today*, **185**, 183 (2012).
8. R. A. Searles, *Stud. Surf. Sci. Catal.*, **116**, 23 (1998)
9. Z. H. Zhou, J. Wang, X. Liu, H. S. O. Chan, *J. Mater. Chem.*, **11**, 1704 (2001)
10. J. Hagen, Industrial Catalysis. A Practical Approach, Wiley-VCH Verlag GmbH & Co. KGaA, Weinheim, Germany, 2006, p. 227.
11. J. H. Scofield, *J. Electron Spectrosc. Relat. Phenom.*, **8**, 129 (1976)
12. W. K. Jozwiak, E. Kaczmarek, T. P. Maniecki, W. Ignaczak, W. Maniukiewicz, *Appl. Catal.*, A, **326**, 17 (2007).
13. Cl. Bianchi, *Catal. Lett.*, **76**, 155 (2001).
14. H. Duan, D. Xu, W. Li, H. Xu, *Catal. Lett.*, **124**, 318 (2008).
15. B. S. Randhawa, H. S. Dosanjh, M. Kaur, *Ceram. Int.*, **35**, 1045 (2009).
16. B. G. Toksha, S. E. Shirsath, S. M. Patange, K. M. Jadhav, *Solid State Commun.*, **147**, 479 (2008).
17. S. Gota, E. Guiot, M. Henriot, M. Gautier-Soyer., *Phys. Rev.* B, **60**, 14387 (1999).
18. A. de la Peña, M. C. Alvarez-Galvan, J. L. G. Fierro, P. L. Arias*, Appl. Catal.* B, **57**, 191 (2005).
19. V. A. de la Peña O'Shea, M. C. Alvarez-Galvan, J. Requies, V. L. Barrio, P. L. Arias, J. F. Cambra, M. B. Güemez, J. L. G. Fierro*, Catal. Commun.*, **8**, 1287 (2007).
20. T. L. Barr, *J. Phys. Chem.*, **82** 1801 (1978).
21. L. Liu, F. Zhou, L.Wang, X. Qi, F. Shi, Y. Deng, *J. Catal.*, **274**, 1–10 (2010).
22. T. Engel, G. Ertl, Oxidation of Carbon Monoxide, in: The Chemical Physics of Solid Surfaces and Heterogeneous Catalysis, D. A. King, D. P. Woodruff (eds.), Elsevier, Amsterdam-Oxford-New York, 1983, vol. 2.

НАНОРАЗМЕРЕН ЖЕЛЕЗЕН ОКСИД С КОНТРОЛИРАН РАЗМЕР, МОДИФИЦИРАН С Pd ЗА ПРОЦЕСИ НА ОЧИСТВАНЕ

С. Ж. Тодорова[1]*, З. П. Черкезова-Желева[1], Ил. Д. Йорданова[1],
А. Гангули[4], Х. Г. Колев[1], С. Мондал[2], М. Г. Шопска[1], К. К. Тенчев[1],
Н. Ив. Велинов[1], А. К. Гангули[2,3,4], Г. Б. Кадинов[1]

[1] Институт по катализ, Българска академия на науките, ул. „Акад. Г. Бончев“, бл. 11, 1113 София, България
[2] Факултет по химия, Индийски технологичен институт, Хаус Кназ, Ню Делхи, 110016, Индия
[3] Факултет за разработки и изследвания на нанотехнологии, Индийски технологичен институт, Хаус Кназ, Ню Делхи, 110016, Индия
[4] Институт по нанонауки и технологии, Мохали, Пенждаб, 160062, Индия

(Резюме)

Получен е наноразмерен Fe_3O_4 от водни разтвори на железни соли посредством утаяване. Така приготвеният оксид е накален и модифициран с паладий. Получените образци са характеризирани чрез методите на рентгеновата дифракция, рентгеновата фотоелектронна спектроскопия, трансмисионната електронна микроскопия, температурно-програмираната редукция и дифузно-отражателната инфрачервена спектроскопия.

Каталитичното поведение на получените материали е изследвано в реакцията на окисление на CO. Установено е силно взаимодействие между паладия и наноразмерния оксид, което води до формирането на финодисперсен PdO на повърхността на образеца. Pd/Fe_2O_3 показва висока каталитична активност в изследваната реакция. Това се обяснява със способността на железния оксид, намиращ се в непосредствена близост до паладия, да доставя активен кислород, който в последствие да реагира с адсорбираните върху Pd молекули CO. Предполага се, че окислението на CO при температури до 100 °C в присъствие на катализатор Pd/Fe_2O_3 протича по механизма на Лангмюир-Хиншелвуд включващ линейно и мостово свързани с паладия молекули CO.